INT program: Intersection of nuclear structure and high-energy nuclear collisions

Probing neutron-skin thickness with free spectator nucleons in ultracentral relativistic heavy-ion collisions

Lu-Meng Liu (刘鹿蒙)
University of Chinese Academy of Sciences (UCAS)
liulumeng18@mails.ucas.ac.cn

February 2023

Collaborators
Tongji University: Jun Xu
Stony Brook University: Jiangyong Jia, Chunjian Zhang

Catalog

Spectator in relativistic HIC: motivation

N_n: number of free spectator neutrons
N_p: number of free spectator protons
L: slope parameter of symmetry energy
$\Delta r_{\rm np} = \langle r_n^2 \rangle^{1/2} - \langle r_p^2 \rangle^{1/2}$: neutron-skin thickness

Density functional theory

$\frac{N_n(^{96}\mathrm{Zr})}{N_n(^{96}\mathrm{Ru})} \sim \Delta r_{np} \sim L$

A **significant enhancement** of N_n in ^{96}Zr + ^{96}Zr collision relative to ^{96}Ru +^{96} Ru collision.
STAR, PRC 105, 014901 (2022)

$\Delta r_{\rm np}(^{96}\mathrm{Zr}) > \Delta r_{\rm np}(^{96}\mathrm{Ru})$

N_n, easily measurable by the ZDC, is sensitive to $\Delta r_{\rm np}$.

In UCC region, most spectator nucleons originate from the surface.

The spectator matter ($v \sim 1$) disconnected from the participant matter at $\sqrt{s_{\rm NN}} = 200$ GeV.

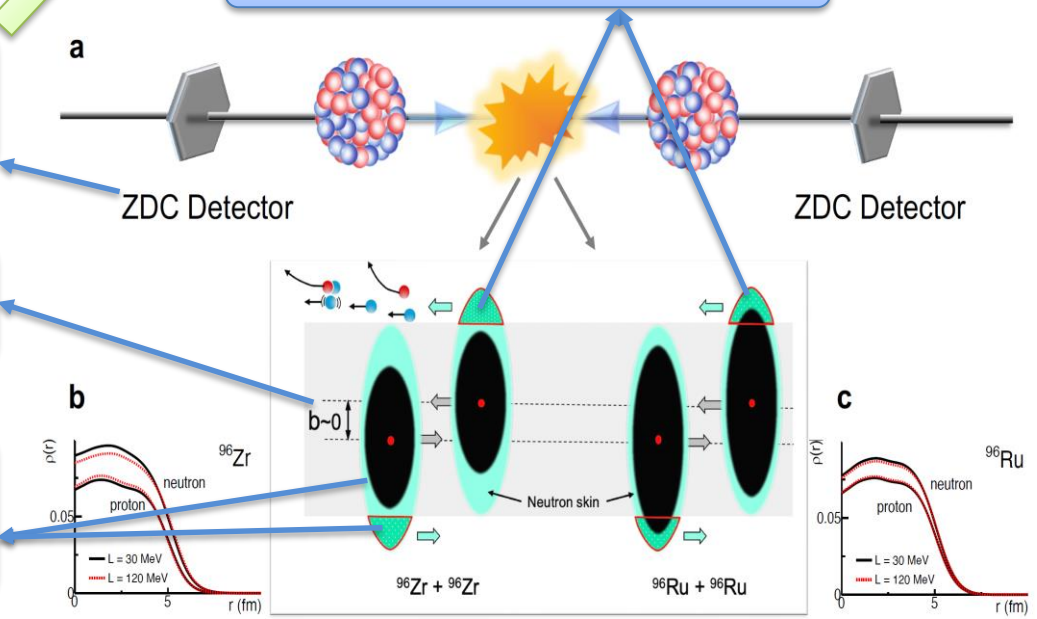

Spectator in relativistic HIC: deexcitation

- Intermediate-energy heavy-ions collision

- High-energy heavy-ions collision

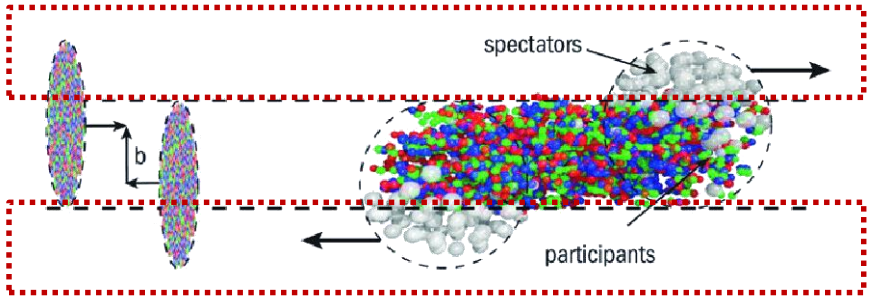

There is almost no interaction between spectator and participant.

- GEMINI model

A Monte Carlo model to calculate the deexcitation of nuclear fragments

R. J. Charity et al., NPA (1988); PRC (2010)

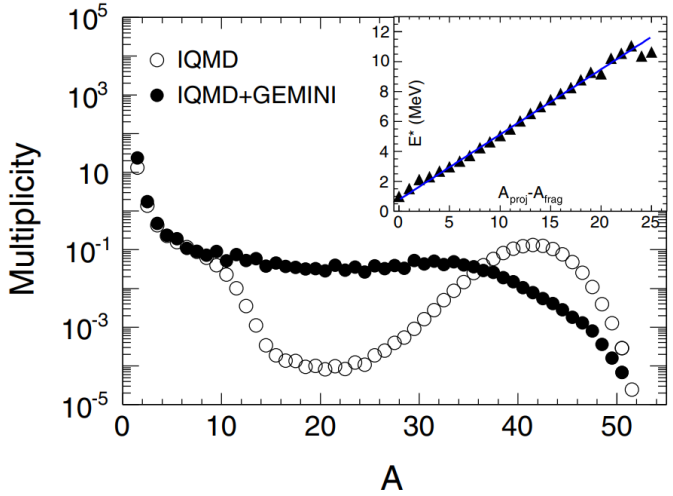

Z. T. Dai, D. Q. Fang, Y. G. Ma et al., PRC (2015)

Spectator in relativistic HIC: deexicitation

- Intermediate-energy heavy-ions collision

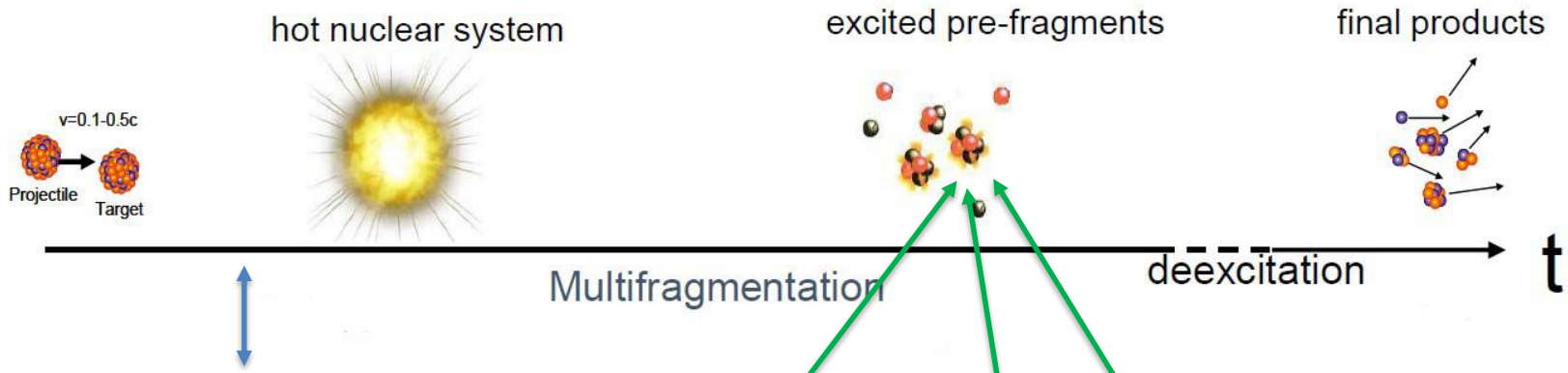

- High-energy heavy-ions collision

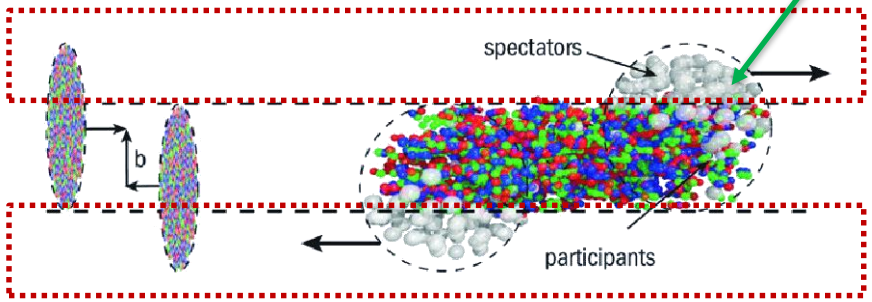

There is almost no interaction between spectator and participant.

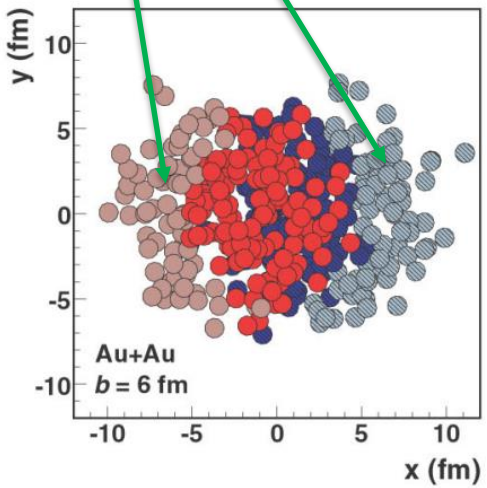

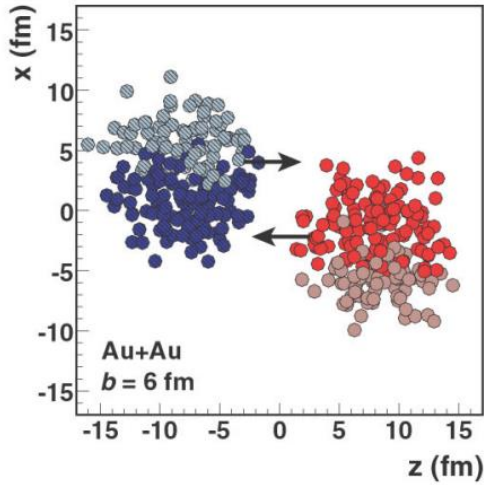

Spectator in relativistic HIC: framework

Framework

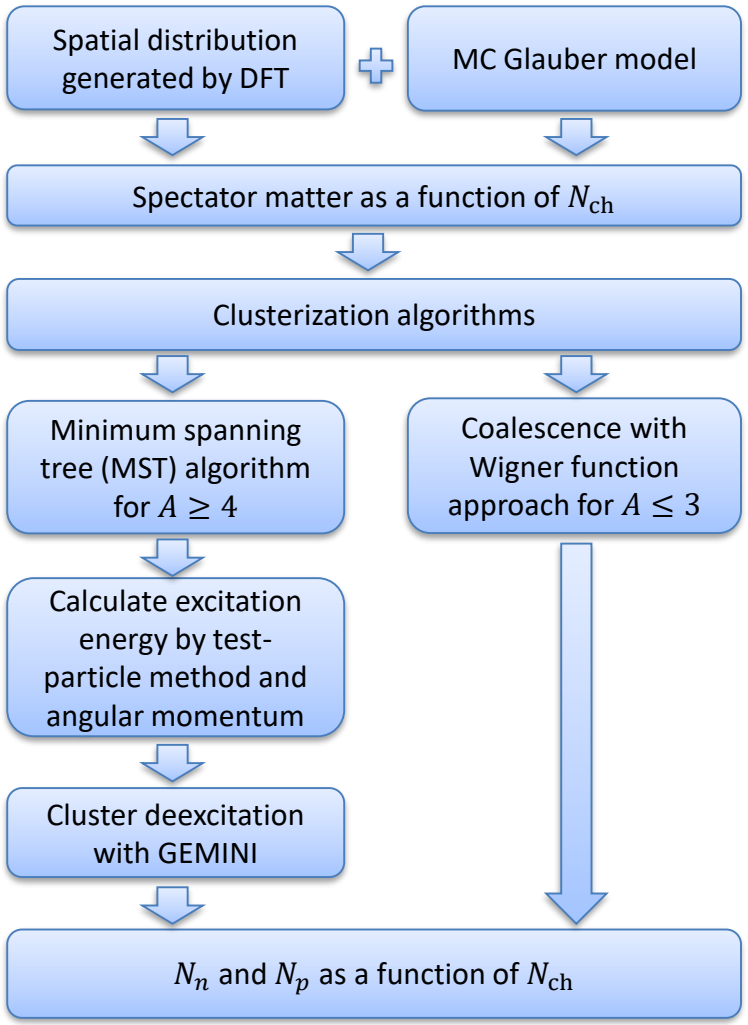

- N_n, as a routine measurement in heavy-ion experiments, is mostly used to estimate the event centrality or the reaction plane.
- Our study is the first to use the N_n to probe the collective structure of colliding nuclei.

Spectator in relativistic HIC: initial density distribution

Skyrme-Hartree-Fock (SHF) model:

Skyrme nuclear force

$$
\begin{aligned}
v(\vec{r}_1,\vec{r}_2) &= t_0(1+x_0P_\sigma)\delta(\vec{r}) \\
&+ \frac{1}{2}t_1(1+x_1P_\sigma)[\vec{k}'^2\delta(\vec{r})+\delta(\vec{r})\vec{k}^2] \\
&+ t_2(1+x_2P_\sigma)\vec{k}'\cdot\delta(\vec{r})\vec{k} \\
&+ \frac{1}{6}t_3(1+x_3P_\sigma)\rho^\alpha(\vec{R})\delta(\vec{r}) \\
&+ iW_0(\vec{\sigma}_1+\vec{\sigma}_2)[\vec{k}'\times\delta(\vec{r})\vec{k}].
\end{aligned}
$$

Hartree-Fock approximation

Energy-density functional

$$
\begin{aligned}
H(\mathbf{r}) = {} & \frac{\hbar^2}{2m}\tau + \frac{1}{2}t_0\left[\left(1+\frac{1}{2}x_0\right)\rho^2 - \left(\frac{1}{2}+x_0\right)\sum_q\rho_q^2\right] \\
& + \frac{1}{2}t_1\left[\left(1+\frac{1}{2}x_1\right)\rho\left(\tau-\frac{3}{4}\Delta\rho\right) - \left(\frac{1}{2}+x_1\right)\sum_q\rho_q\left(\tau_q-\frac{3}{4}\Delta\rho_q\right)\right] \\
& + \frac{1}{2}t_2\left[\left(1+\frac{1}{2}x_2\right)\rho\left(\tau+\frac{1}{4}\Delta\rho\right) - \left(\frac{1}{2}+x_2\right)\sum_q\rho_q\left(\tau_q+\frac{1}{4}\Delta\rho_q\right)\right] \\
& + \frac{1}{12}t_3\rho^\alpha\left[\left(1+\frac{1}{2}x_3\right)\rho^2 - \left(x_3+\frac{1}{2}\right)\sum_q\rho_q^2\right] \\
& - \frac{1}{8}(t_1x_1+t_2x_2)\sum_{ij}\mathbf{J}_{ij}^2 + \frac{1}{8}(t_1-t_2)\sum_{q,ij}\mathbf{J}_{q,ij}^2 - \frac{1}{2}W_0\sum_{ijk}\varepsilon_{ijk}\left[\rho\nabla_k\mathbf{J}_{ij} + \sum_q\rho_q\nabla_k\mathbf{J}_{q,ij}\right]
\end{aligned}
$$

L. W. Chen et al., PRC 82, 024321 (2010)

Skyrme parameters

Quantity	MSL0
t_0 (MeV fm^5)	−2118.06
t_1 (MeV fm^5)	395.196
t_2 (MeV fm^5)	−63.953 1
t_3 (MeV fm$^{3+3\sigma}$)	128 57.7
x_0	−0.070 949 6
x_1	−0.332 282
x_2	1.358 30
x_3	−0.228 181
σ	0.235 879
W_0 (MeV fm^5)	133.3

parameter space transform

macroscopic quantities

Quantity	MSL0
ρ_0 (fm^{-3})	0.16
E_0 (MeV)	−16.0
K_0 (MeV)	230.0
$m^*_{s,0}/m$	0.80
$m^*_{v,0}/m$	0.70
$E_{\rm sym}(\rho_0)$ (MeV)	30.0
L (MeV)	60.0
G_S (MeV fm^5)	132.0
G_V (MeV fm^5)	5.0
$G'_0(\rho_0)$	0.42

variation principle

Self-consistent wave function to the Schrödinger equation:

$$
\left[-\nabla\cdot\frac{\hbar^2}{2m_q^*(\boldsymbol{r})}\nabla + U_q(\boldsymbol{r}) + \boldsymbol{W}_q(\boldsymbol{r})(-i)\cdot\nabla\times\boldsymbol{\sigma}\right]\phi_i(\boldsymbol{r}) = e_i\phi_i(\boldsymbol{r})
$$

Spectator in relativistic HIC: initial density distribution

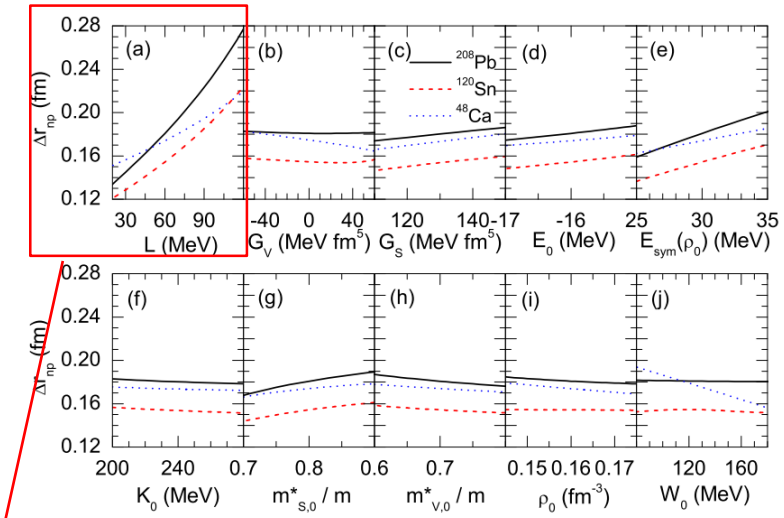

L. W. Chen et al., PRC 82, 024321 (2010)

Δr_{np} depends mostly on L and slightly on other macroscopic quantities.

L. W. Chen et al., PRC 82, 024321 (2010)

Skyrme parameters

Quantity	MSL0
t_0 (MeV fm^5)	−2118.06
t_1 (MeV fm^5)	395.196
t_2 (MeV fm^5)	−63.953 1
t_3 (MeV fm$^{3+3\sigma}$)	128 57.7
x_0	−0.070 949 6
x_1	−0.332 282
x_2	1.358 30
x_3	−0.228 181
σ	0.235 879
W_0 (MeV fm^5)	133.3

parameter space transform

macroscopic quantities

Quantity	MSL0
ρ_0 (fm^{-3})	0.16
E_0 (MeV)	−16.0
K_0 (MeV)	230.0
$m^*_{s,0}/m$	0.80
$m^*_{v,0}/m$	0.70
$E_{\rm sym}(\rho_0)$ (MeV)	30.0
L (MeV)	60.0
G_S (MeV fm^5)	132.0
G_V (MeV fm^5)	5.0
$G'_0(\rho_0)$	0.42

Slope parameter $L = 3\rho_0 \left[\frac{\partial E_{sym}(\rho)}{\partial \rho}\right]_{\rho=\rho_0}$ Symmetry energy; Saturation density

Neutron skin $\Delta r_{\rm np} = \langle r_n^2 \rangle^{1/2} - \langle r_p^2 \rangle^{1/2}$

Spectator in relativistic HIC: initial density distribution

Slope parameter

B. A. Li and X. Han, PLB (2013)
M. Oertel et al., RMP (2017)

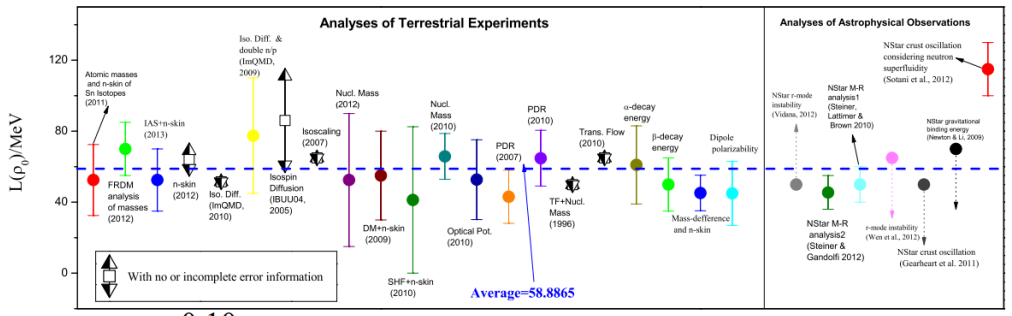

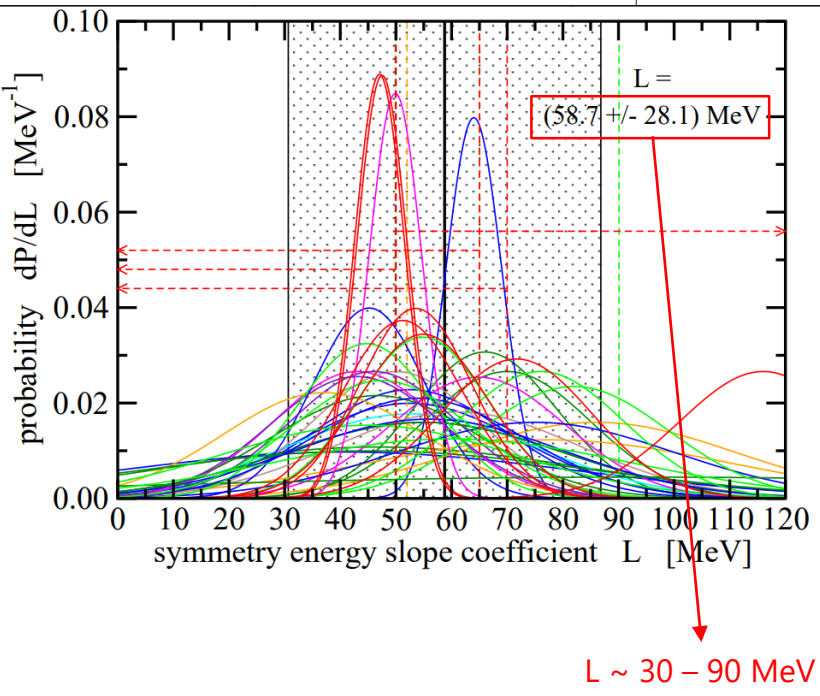

L ~ 30 – 90 MeV

PREXII data of ^{208}Pb favors a large $L(\rho_0) = (106 \pm 37)$ MeV

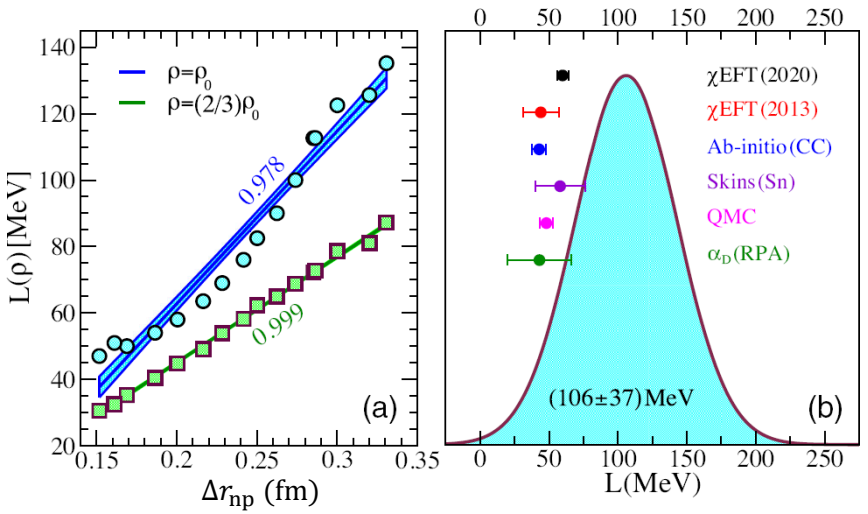

$\Delta r_{np}^{Pb} = (0.284 \pm 0.071)$ fm
B. T. Reed et al., PRL 126, 172503 (2021)

L ~ 30 - 120 MeV

Deformed nucleus

Skyrme-Hartree–Fock–Bogoliubov (SHFB) method using the cylindrical transformed deformed harmonic oscillator basis.
M. V. Stoitsov et al., CPC (2013)

Constrained multipole moments

$$\beta_{\lambda,\tau} = \frac{4\pi Q_{\lambda,\tau}}{3N_\tau R^\lambda}$$

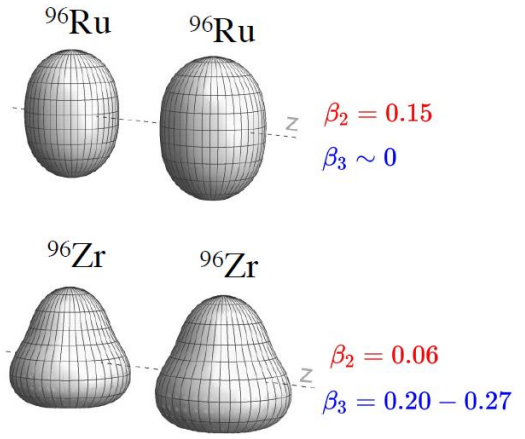

C. Zhang and J. Jia, PRL 128, 022301 (2022)
J. Jia, PRC 105, 014905 (2022)

Spectator in relativistic HIC: Monte-Carlo Glauber model

Two-component Glauber model

Number of source

$$N_{\mathrm{s}} = (1-x)\frac{N_{\mathrm{part}}}{2} + xN_{\mathrm{coll}}$$

Negative binomial distribution

$$p_{\mathrm{nbd}}(n;m,p) = \frac{(n+m-1)!}{(m-1)!n!}p^n(1-p)^m$$

NN inelastic cross section

$\sqrt{s_{NN}}$	130 GeV	200 GeV	5.02 TeV
σ_{NN}	40 mb	42 mb	68 mb

Parameters

	$\sqrt{s_{\mathrm{NN}}}$	x	$\bar{n}$	m
$^{96}\mathrm{Zr}+^{96}\mathrm{Zr}$	200 GeV	0.12	2.3	2.0
$^{96}\mathrm{Ru}+^{96}\mathrm{Ru}$	200 GeV	0.12	2.3	2.2
$^{197}\mathrm{Au}+^{197}\mathrm{Au}$	130 GeV	0	4.8	4.6
$^{197}\mathrm{Au}+^{197}\mathrm{Au}$	200 GeV	0.10	5.8	2.3
$^{208}\mathrm{Pb}+^{208}\mathrm{Pb}$	5.02 TeV	0.09	10.3	3.2

N_{ch} fitting

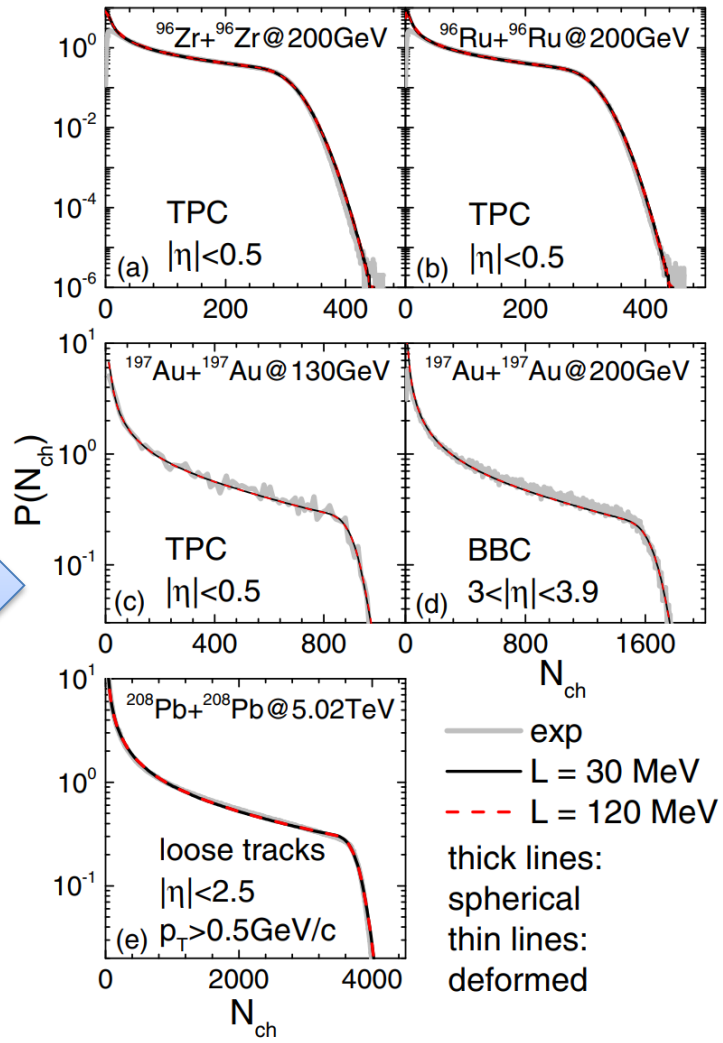

Observables as a function of charged-particle multiplicity N_{ch}

Spectator in relativistic HIC: clusterization and deexcitation

A. Heavy clusters with $A \geq 4$ handled by the minimum spanning tree (MST) algorithm

coalescence parameter (fitted by the Au + Au data)

$\Delta r_{\max} = 3$ fm (empirical nucleon interaction range)
$\Delta p_{\max} = 300$ MeV/c (empirical Fermi momentum at ρ_0)

Formed clusters

Excitation energy

$$E = \frac{1}{N_{TP}} \sum_i \left(\sqrt{m^2 + p_i^2} - m \right)$$

Simplified SHF EDF (test-particle method for parallel events with similar collision configuration)

$$+ \int d^3r \left[\frac{a}{2} \left(\frac{\rho}{\rho_0} \right)^2 + \frac{b}{\sigma + 1} \left(\frac{\rho}{\rho_0} \right)^{\sigma+1} \right]$$
$$+ \int d^3r E_{\text{sym}}^{\text{pot}} \left(\frac{\rho}{\rho_0} \right)^{\gamma} \frac{(\rho_n - \rho_p)^2}{\rho}$$
$$+ \int d^3r \left\{ \frac{G_S}{2} (\nabla \rho)^2 - \frac{G_V}{2} [\nabla (\rho_n - \rho_p)]^2 \right\}$$
$$+ \frac{e^2}{2} \int d^3r d^3r' \frac{\rho_p(\vec{r}) \rho_p(\vec{r}')}{|\vec{r} - \vec{r}'|} - \frac{3e^2}{4} \int d^3r \left[\frac{3\rho_p}{\pi} \right]^{4/3} - E_{GS}$$

Angular momentum $\vec{L} = \sum_i \vec{r}_i \times \vec{p}_i$

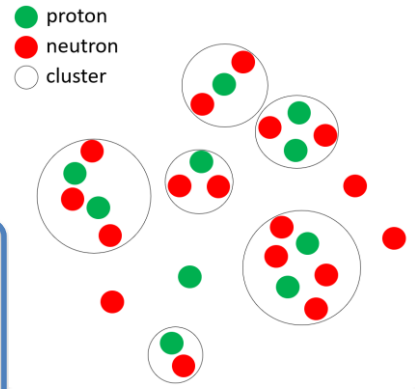

A and B are two sources of free spectator nucleons

Heavy cluster deexcitation with GEMINI model with the input parameters of mass number A, proton number Z, excitation energy and angular momentum.

The free spectator nucleons from the deexcitation

B. Other spectator nucleons coalesce into light clusters with $A \leq 3$ according Wigner functions

$$f_d = 8 g_d \exp\left(-\frac{\rho^2}{\sigma_d^2} - p_\rho^2 \sigma_d^2 \right),$$

$$f_{t/^3He} = 8^2 g_{t/^3\text{He}} \exp\left[-\left(\frac{\rho^2 + \lambda^2}{\sigma_{t/^3\text{He}}^2} \right) - (p_\rho^2 + p_\lambda^2) \sigma_{t/^3\text{He}}^2 \right],$$

The residue nucleons that have not coalesced into light clusters

Total free spectator neutrons N_n and protons N_p

Spectator in relativistic HIC: results

1. Density distribution

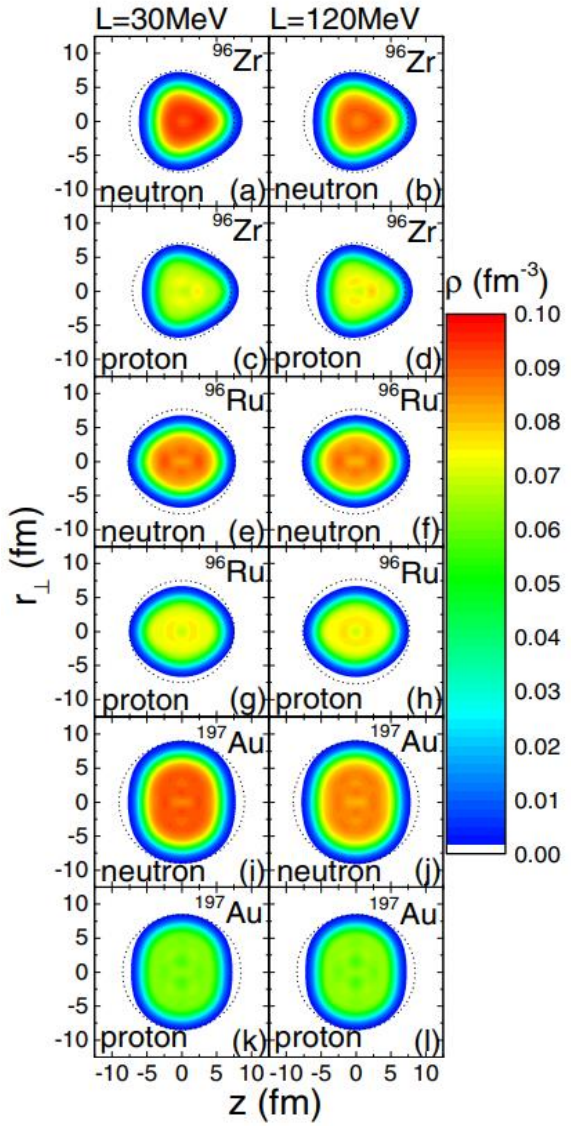

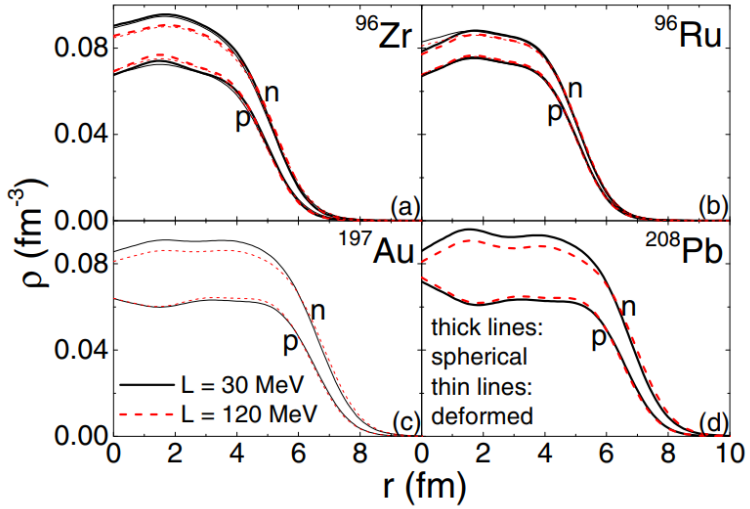

2. Validation with experimental data

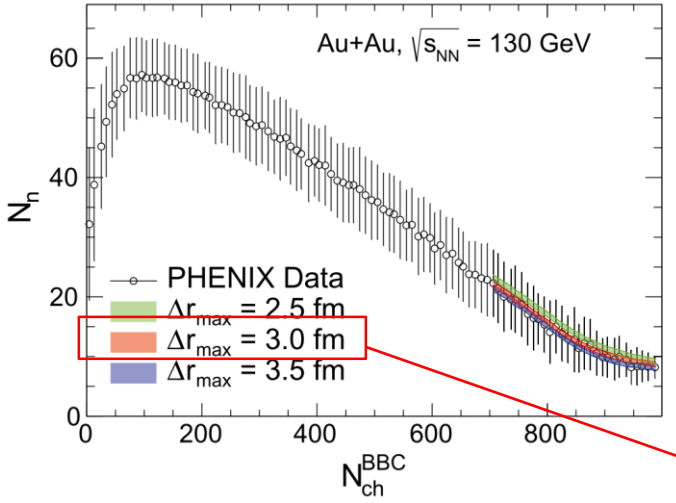

The value of $\Delta r_{\max} = 3$ fm achieves the best description

Spectator in relativistic HIC: predictions

1. Bulk properties of spectator matter

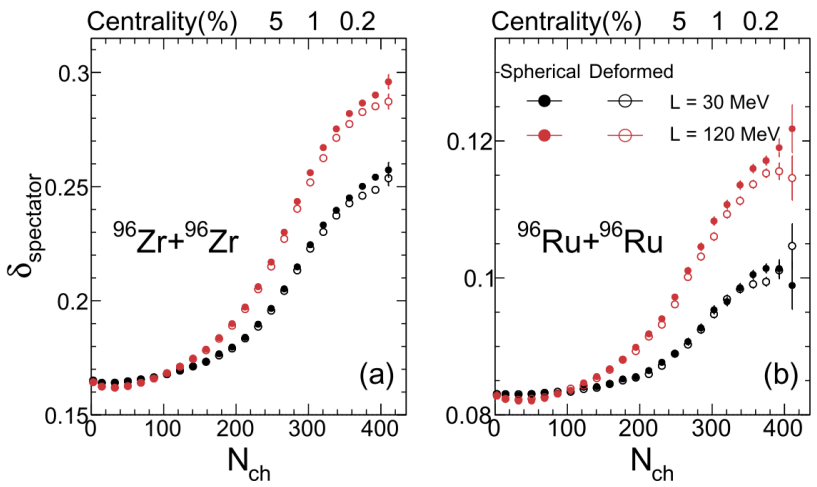

2. Predictions for the isobar systems

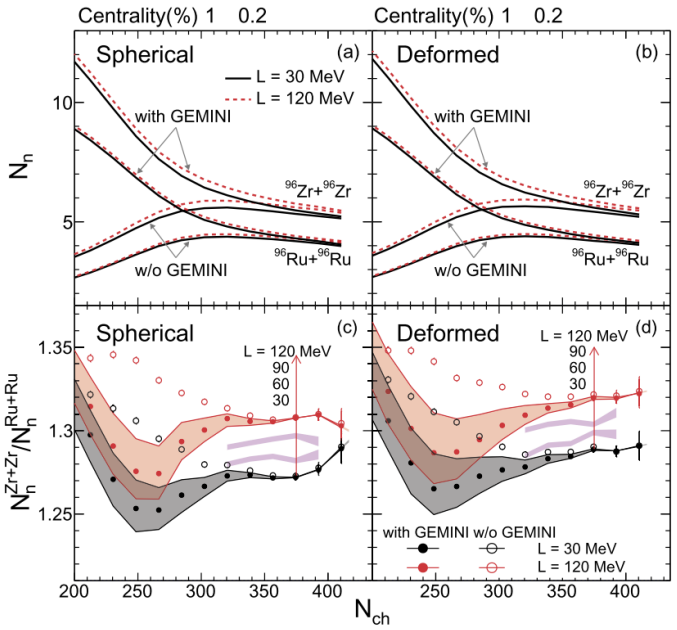

3. Predictions for different collision systems

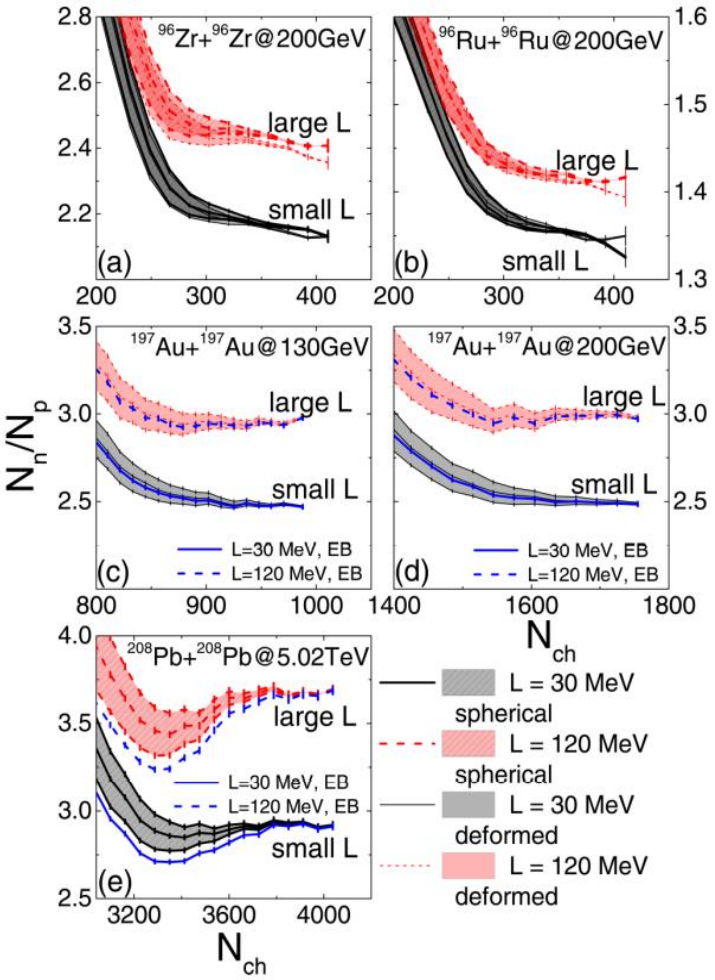

- **L.-M. Liu**, C. Zhang, J. Zhou, J. Xu*, J. Jia*, and G.-X. Peng, Phys. Lett. B 834, 137441 (2022), arXiv:2203.09924 [nucl-th].
- **L.-M. Liu**, C. Zhang, J. Xu*, J. Jia*, and G.-X. Peng, Phys. Rev. C 106, 034913 (2022), arXiv:2209.03106 [nucl-th].

Spectator in relativistic HIC: spin-orbit coupling

Spin-orbit coupling

$$v_{so} = iW_0(\vec{\sigma}_1 + \vec{\sigma}_2) \cdot \vec{k}' \times \delta(\vec{r}_1 - \vec{r}_2)\vec{k}$$

Deformation

$$Q_{\lambda,\tau} = \int \rho_\tau(\vec{r}) r^\lambda Y_{\lambda 0}(\theta) d^3r$$

- Polar angular distributions of the neutron skin

$$\Delta r_{\rm np}(\Omega) = \sqrt{\langle r_{\rm n}^2(\Omega)\rangle} - \sqrt{\langle r_{\rm p}^2(\Omega)\rangle}$$

$$\sqrt{\langle r_\tau^2(\Omega)\rangle} = \left(\frac{\int \rho_\tau(r,\Omega) r^4 dr}{\int \rho_\tau(r,\Omega) r^2 dr}\right)^{1/2}$$

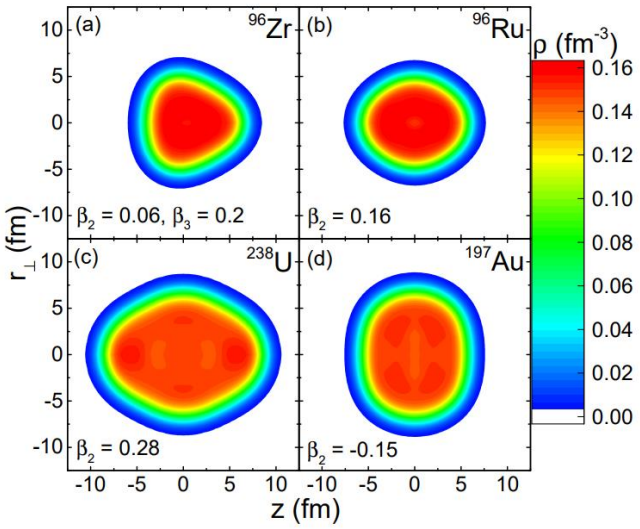

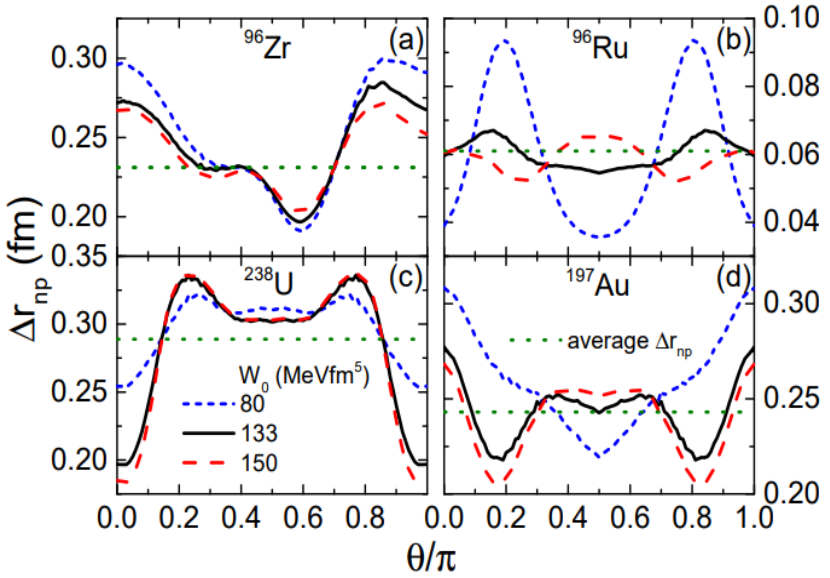

Spectator in relativistic HIC: spin-orbit coupling

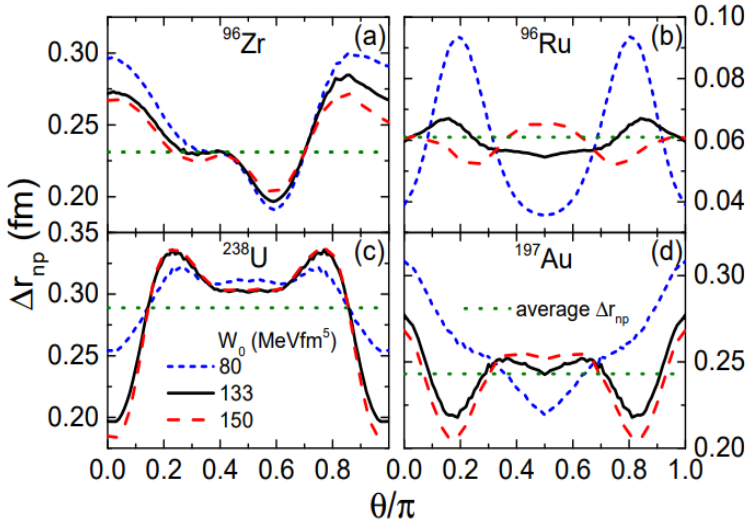

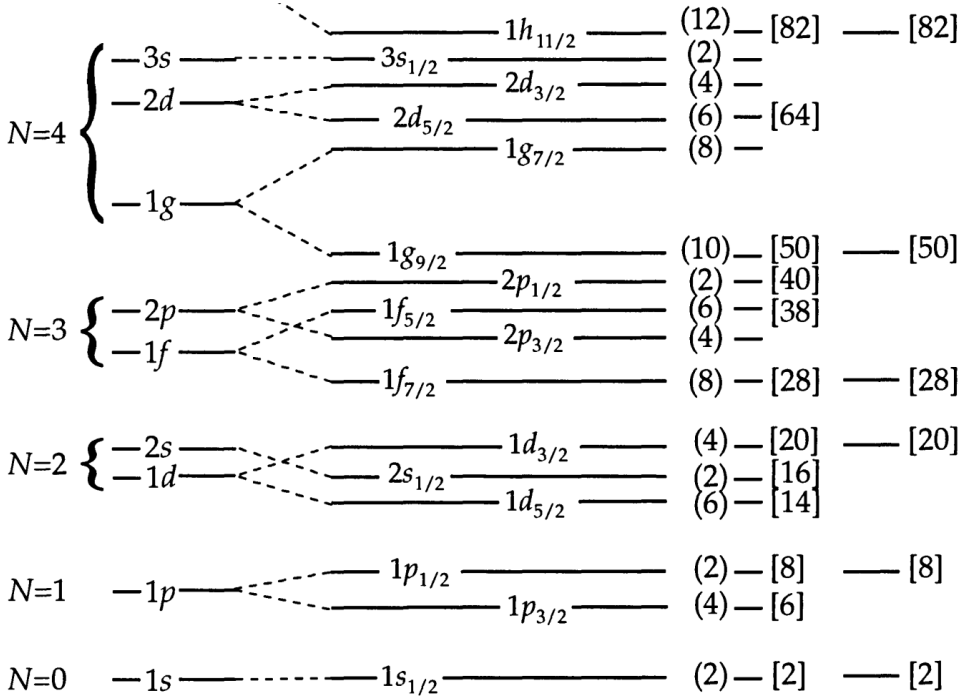

Schematic diagram of energy levels

Spectator in relativistic HIC: spin-orbit coupling

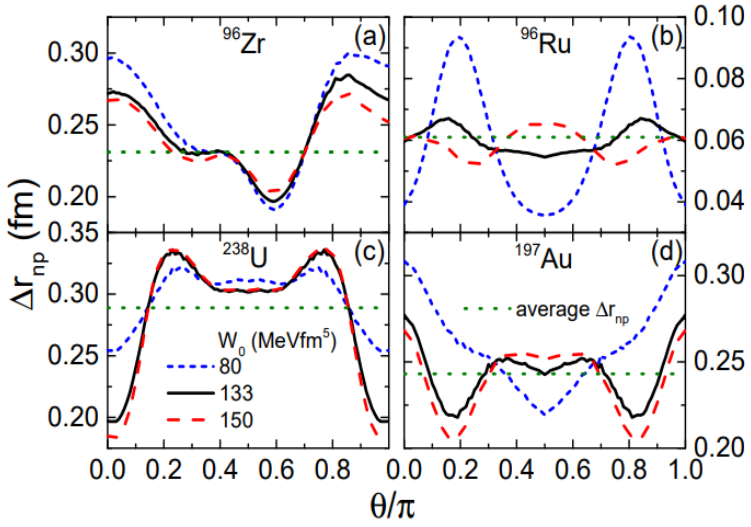

Spin-orbit coupling

$$v_{so} = iW_0(\vec{\sigma}_1 + \vec{\sigma}_2) \cdot \vec{k}' \times \delta(\vec{r}_1 - \vec{r}_2)\vec{k}$$

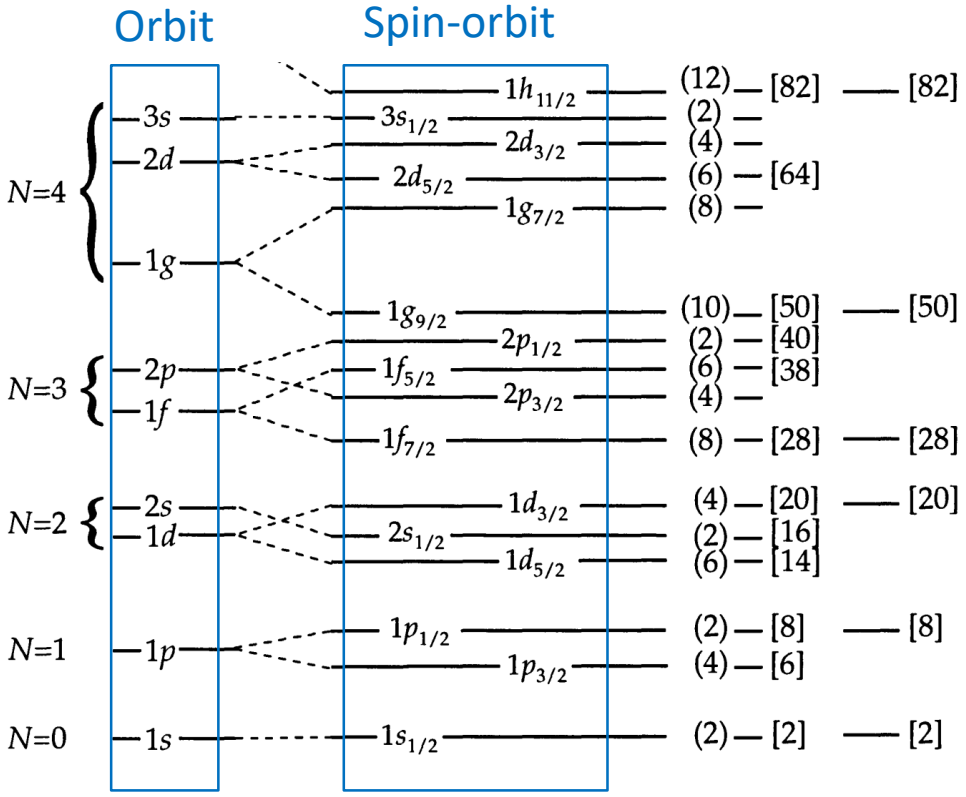

Schematic diagram of energy levels

Spectator in relativistic HIC: spin-orbit coupling

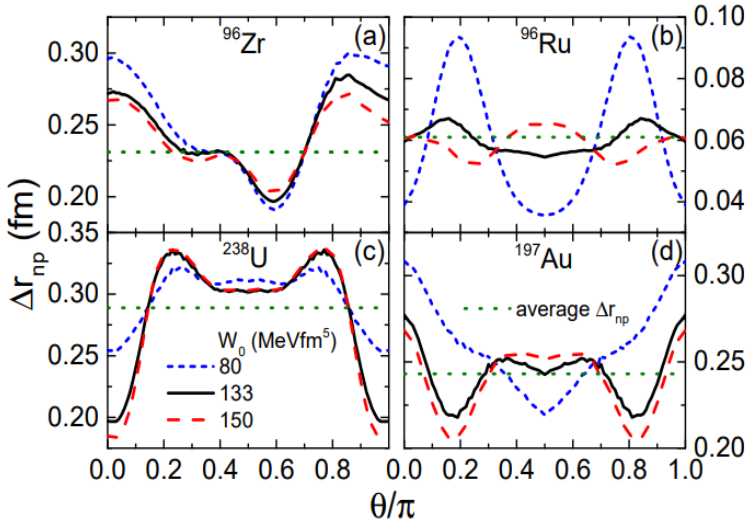

Spin-orbit coupling

$$v_{so} = iW_0(\vec{\sigma}_1 + \vec{\sigma}_2) \cdot \vec{k}' \times \delta(\vec{r}_1 - \vec{r}_2)\vec{k}$$

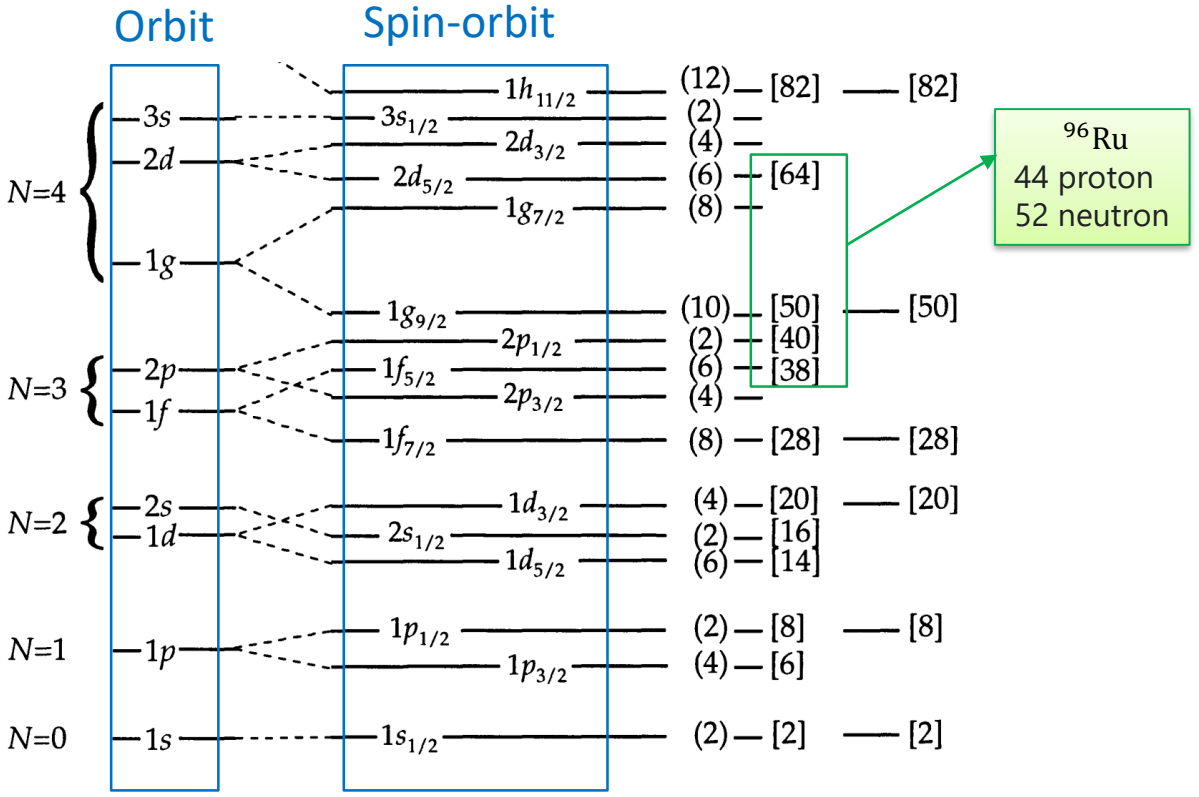

Schematic diagram of energy levels

Spectator in relativistic HIC: spin-orbit coupling

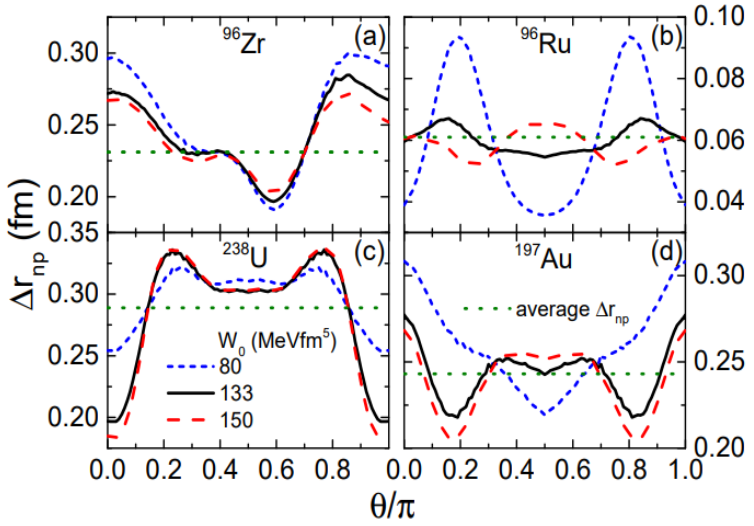

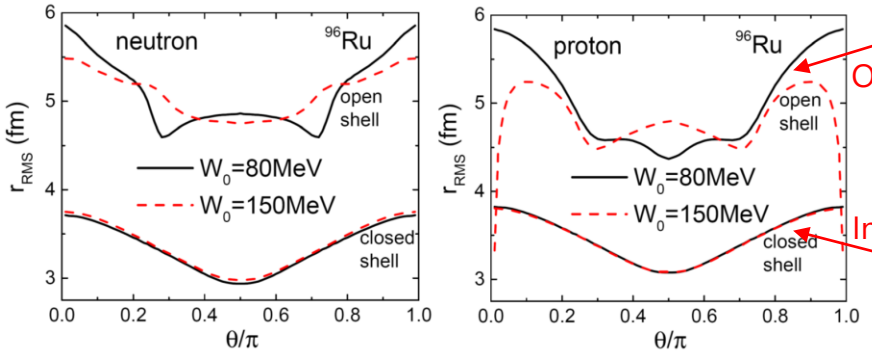

Angular distributions of the RMS radii for typical neutrons (left) and protons (right) in loosely-bound open shells and tightly-bound closed shells of ^{96}Ru using different W_0

Outermost nucleon

Innermost nucleon

Spin-orbit coupling

$$v_{so} = iW_0(\vec{\sigma}_1 + \vec{\sigma}_2) \cdot \vec{k}' \times \delta(\vec{r}_1 - \vec{r}_2)\vec{k}$$

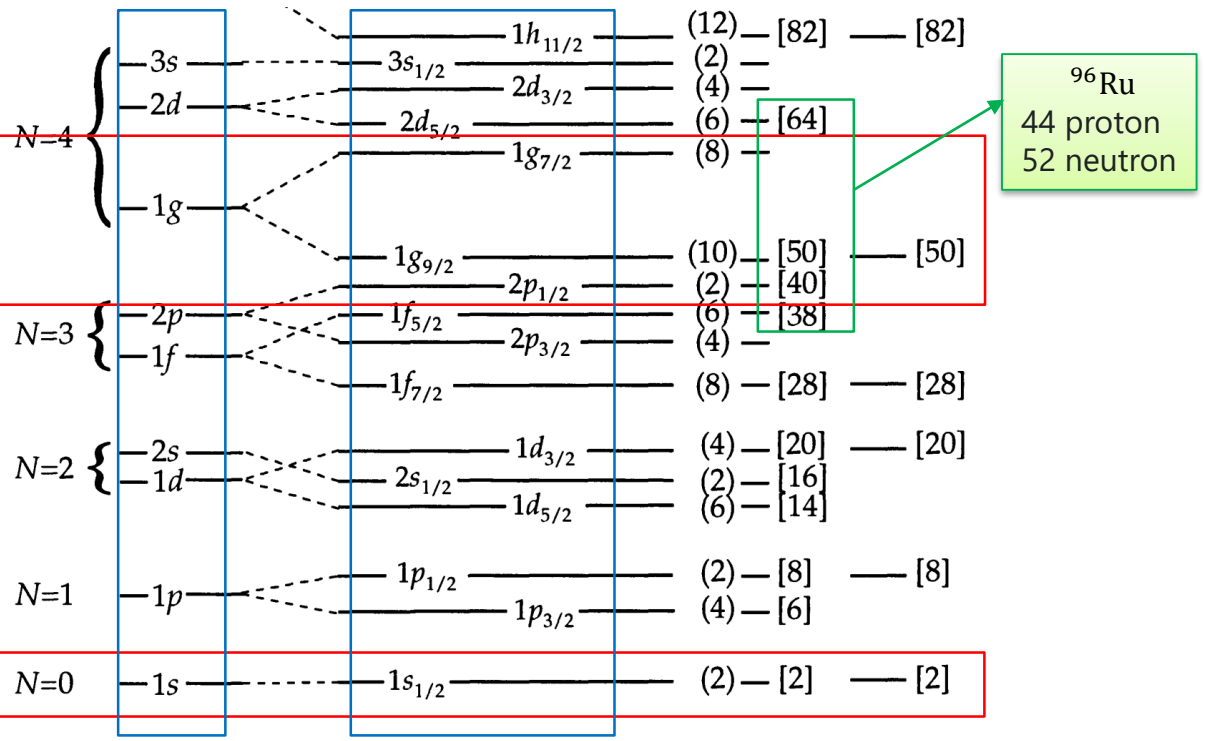

^{96}Ru
44 proton
52 neutron

Schematic diagram of energy levels

Under study…

Spectator in relativistic HIC: predictions

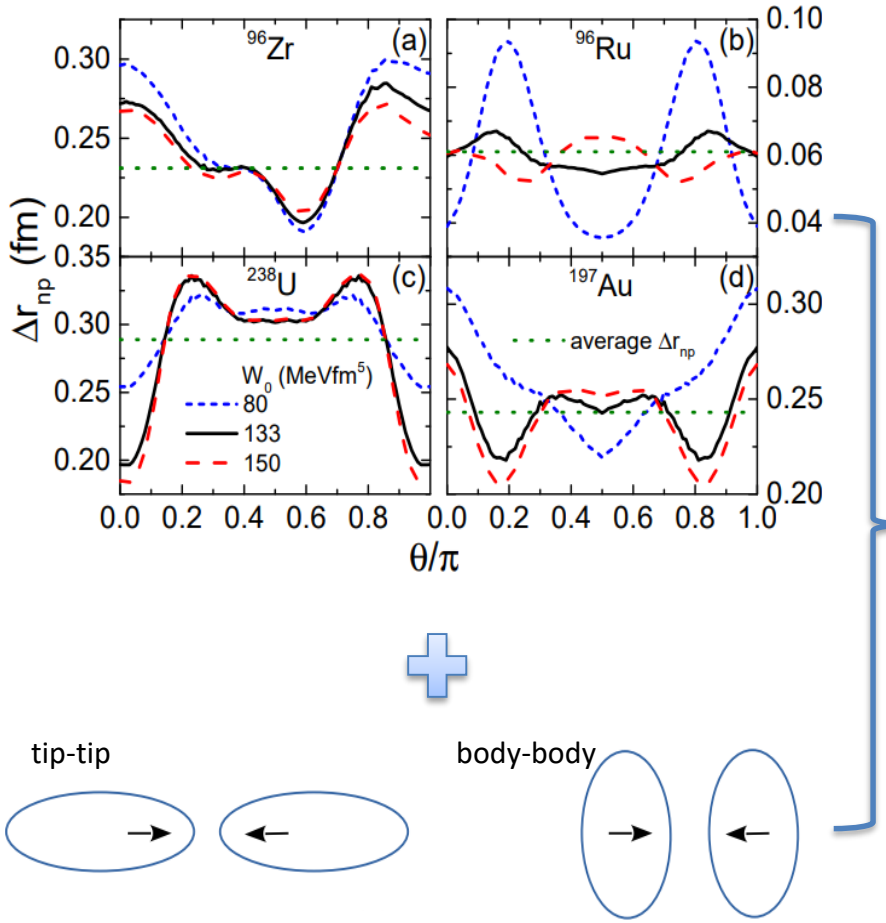

2. Predictions for different collision configurations at C. M. energy $\sqrt{s_{NN}}$ = 200 GeV

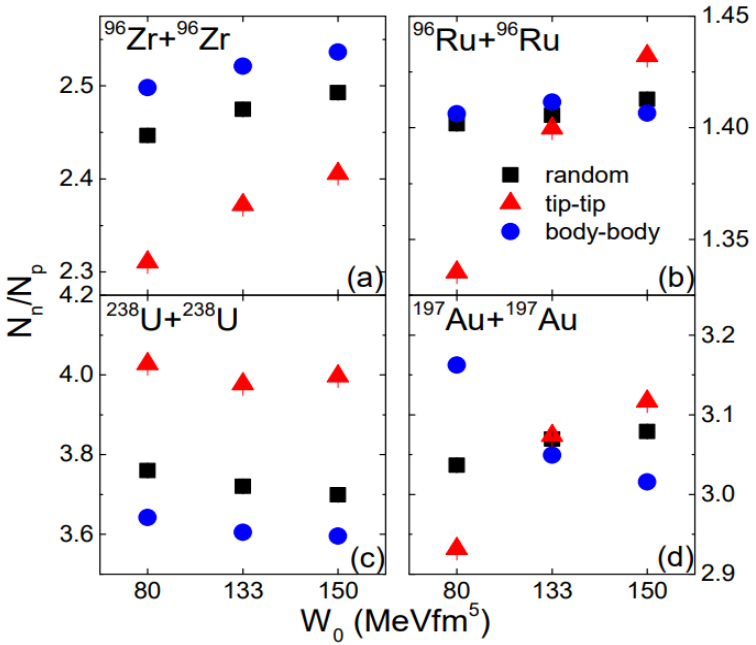

- **L.-M. Liu**, J. Xu*, and G.-X. Peng, , Phys. Lett. B 838, 137701 (2023), arXiv:2301.07893 [nucl-th].
- **L.-M. Liu**, J. Xu*, and G.-X. Peng, to be published in Nucl. Phys. Rev., arXiv:2301.08251 [nucl-th].

Summary and outlook

The yield ratio of free spectator nucleon as a probe of Δr_{np} and W_0

- Spectator nucleons: not suffer from the complex dynamics for observables at midrapidities and easily measurable.
- SHFB: self-consistent spherical and deformed calculations + parameter space transform.
- Ultracentral HIC: free from the uncertainty of deexcitations.
- Ratio of neutron-rich to neutron-poor system: reduce uncertainties.
- Moreover: N_n/N_p ratio is an excellent probe of Δr_{np} and L for a single colliding system.
- Collision configuration: $W_0 \rightarrow \Delta r_{\mathrm{np}}(\Omega) \rightarrow$ different N_n/N_p ratio in different Collision configurations.
- SOC: spin-orbit coupling $W_0 \rightarrow$ outer nucleon RMS $\rightarrow \Delta r_{\mathrm{np}}(\Omega)$? Under study…

Thanks !

Backup: double ratio

Double ratio in the isobar system

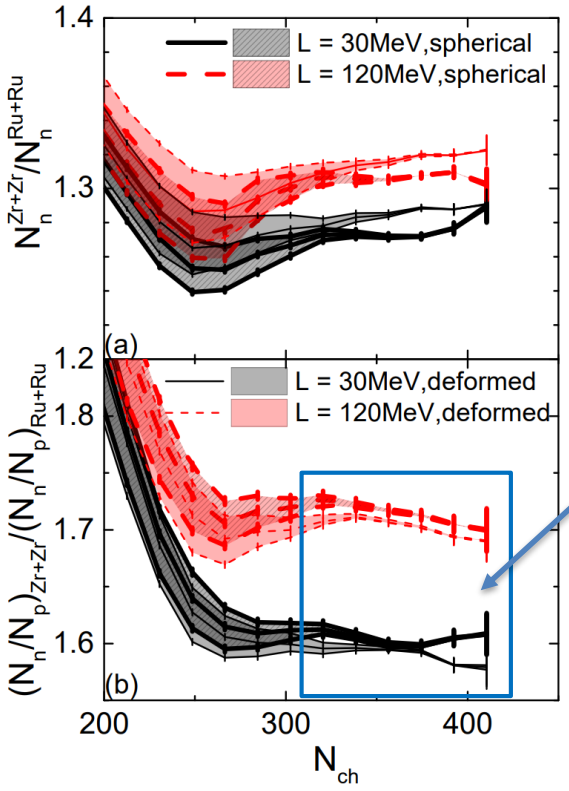

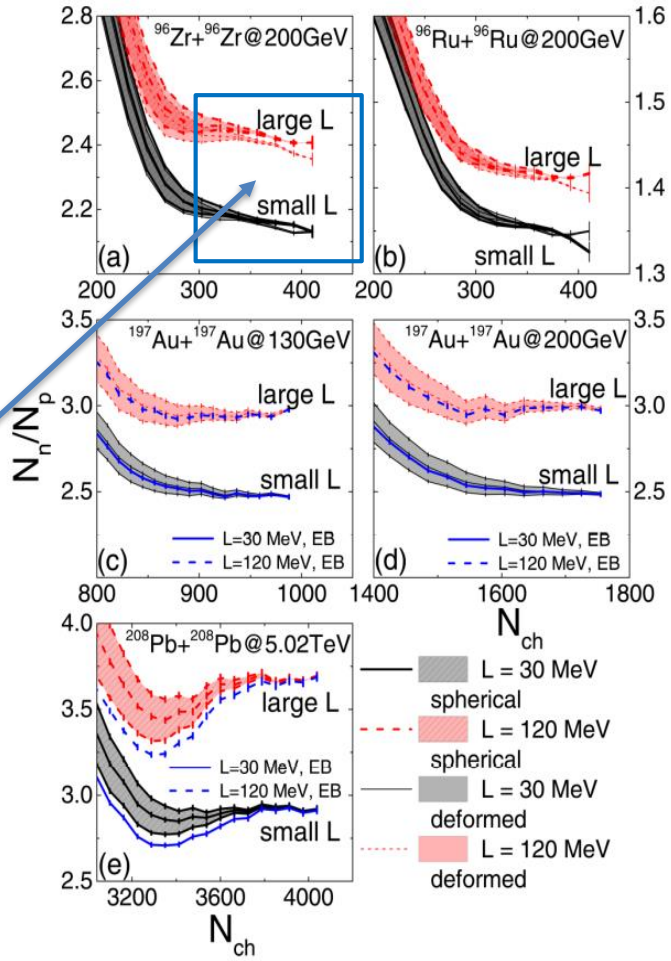

TABLE IV. Yield ratio N_n/N_p of free spectator neutrons to protons in the UCC region of different collision systems and for different slope parameters L (in MeV) of the symmetry energy.

	$\sqrt{s_{NN}}$	β_2, β_3	N_n/N_p	
			$L = 30$	$L = 120$
^{96}Zr+^{96}Zr	200 GeV	0, 0	2.15	2.40
		0.06, 0.2	2.15	2.35
^{96}Ru+^{96}Ru	200 GeV	0, 0	1.35	1.40
		0.16, 0	1.35	1.40
^{197}Au+^{197}Au	130 GeV	-0.15, 0	2.5	3.0
^{197}Au+^{197}Au	200 GeV	-0.15, 0	2.5	3.0
^{208}Pb+^{208}Pb	5.02 TeV	0, 0	2.9	3.7

Take the ratio of the $\frac{N_n(^{96}\mathrm{Zr})}{N_n(^{96}\mathrm{Ru})}$ ratio in the isobaric systems

- The effects of L is a little smaller than that in single collision systems.
- Cancel the detecting efficiency for protons.

Backup: Spectator particle yield

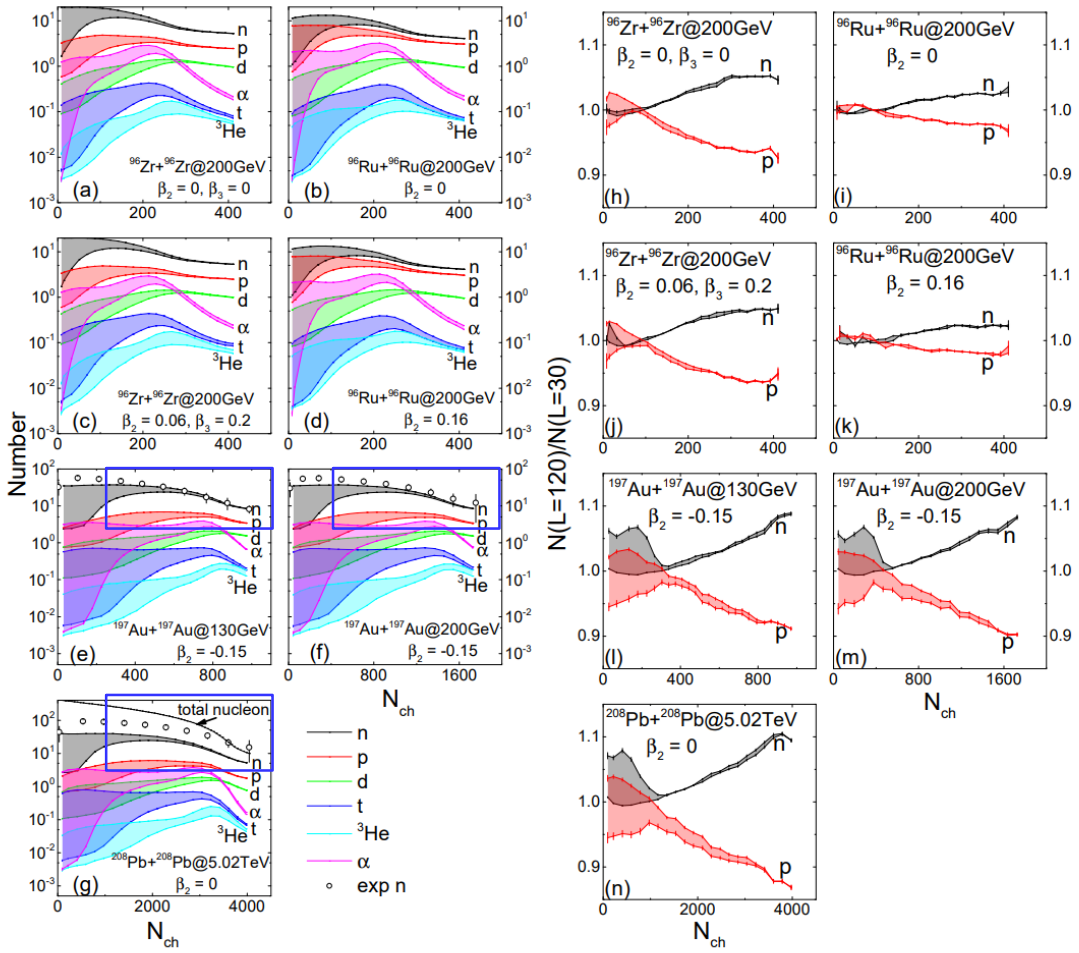

FIG. 6. Left: Numbers of free spectator nucleons and light clusters from ^{96}Zr+^{96}Zr at $\sqrt{s_{\rm NN}}$ = 200 GeV, ^{96}Ru+^{96}Ru at $\sqrt{s_{\rm NN}}$ = 200 GeV, ^{197}Au+^{197}Au at $\sqrt{s_{\rm NN}}$ = 130 GeV, ^{197}Au+^{197}Au at $\sqrt{s_{\rm NN}}$ = 200 GeV, and ^{208}Pb+^{208}Pb at $\sqrt{s_{\rm NN}}$ = 5.02 TeV collision systems for L = 30 MeV and with different deformation parameters. Estimated spectator neutrons from experimental data measured by ZDC in the collisions of ^{197}Au+^{197}Au at $\sqrt{s_{\rm NN}}$ = 130 GeV [69], ^{197}Au+^{197}Au at $\sqrt{s_{\rm NN}}$ = 200 GeV [70], and ^{208}Pb+^{208}Pb at $\sqrt{s_{\rm NN}}$ = 5.02 TeV [37, 71] are also plotted for comparison. Right: Yield ratios of free spectator neutrons and protons for L = 120 MeV to those for L = 30 MeV in the corresponding systems as in the left panels. Bands represent the uncertainty of ±1 MeV per nucleon in calculating the excitation energy for the deexcitation of heavy fragments by GEMINI.

Backup: electromagnetic excitation

Average energy excitation per spectator nucleon
from the electromagnetic field

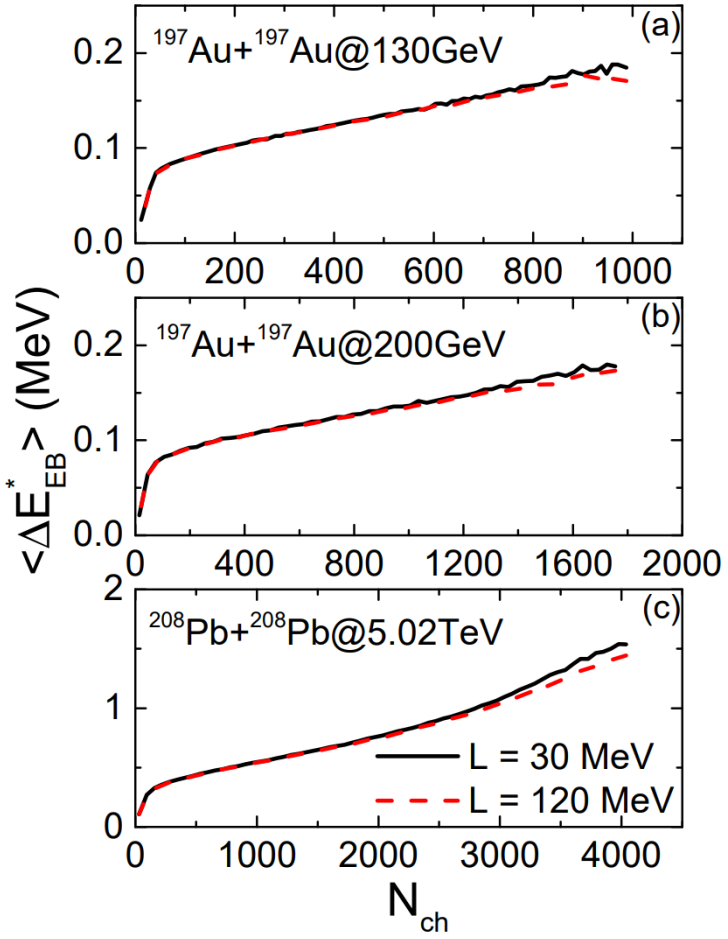

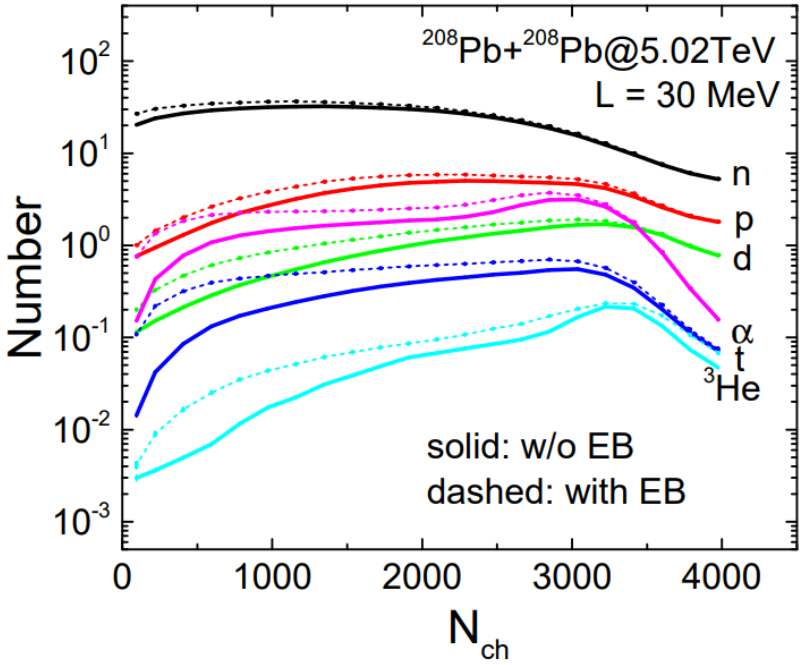

The effects from the electromagnetic field normally smaller than the assumed uncertainty of ± 1 MeV per nucleon that we already considered in calculating the excitation energy of heavy fragments.